Vibrational Level Populations of Hydrogen Fluoride Produced in Infrared Multiple-photon Decompositon of C_2H_5F

Yo-ichi ISHIKAWA* and Shigeyoshi ARAI
The Institute of Physical and Chemical Research, Wako-shi, Saitama 351-01
(Received July 30, 1983)

CO_2 TEA laser-induced photolysis of C_2H_5F was studied by using a time-resolved infrared fluorescence technique. Molecular elimination of vibrationally excited hydrogen fluoride (HF*) from C_2H_5F* occurs in the process. Rotational temperatures and vibrational level populations of HF* are estimated from observed fluorescence spectra by computational fitting. Higher vibrational levels are populated to a less extent in the decomposition under a collisionless condition. When the pressure of C_2H_5F is increased, however, population inversion is allowed among some levels. Possible reaction mechanism is discussed for the production of HF* at extraordinarily high vibrational levels.

Infrared multiple-photon decomposition (IRMPD) is usually considered to be a unimolecular decomposition of a molecule excited vibrationally above its decomposition threshold under a collisionless condition. However, it has been pointed out that the decomposition induced by collisions between highly vibrationally excited molecules occurs significantly even in a relatively low pressure region.[1-3] Previous time-resolved luminescence studies show that both instantaneous and delayed emissions are observable in IRMPD.[1,3,4] The latter has been ascribed to radiative species produced in collisions between highly vibrationally excited molecules. The collision-induced decomposition was estimated to contribute over 90% to the total decomposition at a pressure as low as 0.07 Torr (1 Torr≈133.322 Pa), where excited molecules can not collide with each other at least within a laser pulse duration.[3] On the other hand, Danen and Jang[5] have suggested that the decomposition *via* collisional V-V ladder climbing is not significant in IRMPD of large molecules.

The time-resolved infrared spectroscopic technique has been applied to UV photolysis by an excimer laser[6] or IRMPD by a CO_2 TEA laser.[7-9] This method affords dynamic information on rotation-vibration states of decomposition fragments and parent molecules. Quick and Wittig[8] measured infrared fluorescence spectra of HF* produced in IRMPD of fluorinated ethanes and ethylenes and estimated the rotational temperatures and vibrational distributions from spectral simulation. They found $N_v/N_{v+1}>1$ under a collisionless condition, where N_v and N_{v+1} denote the vibrational level populations at levels v and $v+1$, respectively. The addition of inert gas does not influence the vibrational distribution, while it lowers the rotational temperature.

Our previous study has shown that the energy transfer from highly vibrationally excited molecules is a main cause for isotope scrambling in IRMPD of mixtures of trifluoromethane-d_1 and -d_0 (CDF_3 and CHF_3).[9] However, the kinetic behavior of highly vibrationally excited molecule has not yet been well understood except for its unimolecular decomposition channel.[4,10] In this paper, we report time-resolved infrared fluorescence spectra observed in IRMPD of C_2H_5F, where the pressure of reactant is varied from 0.025 Torr, a collisionless condition, to 10 Torr. The fluorescence in the wavelength region of 2.2—3.2 μm is due to the HF* produced in a molecular elimination process. The role of highly vibrationally excited parent molecule in IRMPD will be discussed on the basis of the estimate of rotational temperatures and vibrational distributions of HF*.

Experimental

The experimental apparatus and procedure are similar to the previous ones.[9] The laser used for irradiation was a CO_2 TEA laser (Lumonics 103-2). The pulse duration was about 80 ns fwhm when the laser was operated without nitrogen gas in the cavity. All samples were irradiated with the P(20) line (1046.85 cm^{-1}) of the 9.6 μm CO_2 band at a repetition rate of 0.7 Hz. Laser energy was measured with a pyroelectric detector. The laser beam was truncated through a 9.9 mm diameter iris and focused onto the center of irradiation cell with a BaF_2 lens ($f.l.$=20 cm). The beam area at focus was estimated to be 5×10^{-3} cm^2 from a beam divergence of about 2 mrad. Laser fluences at focus were calculated from the beam area and laser energies. The cell with two KBr windows at both ends was 36 cm in length in the laser beam direction and 2 cm in inner diameter. The infrared fluorescence light at a focal regime, *i.e.*, in the vicinity of the center of cell, was made parallel by a parabolic mirror and then focused on the entrance slit of the infrared spectrometer (Ritsu Oyo Kogaku, MC-20L) by a CaF_2 lens ($f.l.$=20 cm). The focal point of laser beam was adjusted to fit the focal point of the parabolic mirror in the optical arrangement. More than 70% of the emission light at focus is converted into a parallel beam by reflection on the parabolic mirror. The maximum field of view of the detection system is limited to a 2 cm range along the laser beam within the enclosure of mirror. The fluence variation may be milder than 40% of the fluence at focus because the optical setup was designed to pick up most efficiently the emission in the vicinity of the focus. The infrared light was detected with an InSb detector mounted behind the exit slit of spectrometer. The current signal from the detector, after converted into a voltage signal, was amplified by a preamplifier (PAR Model 115) and then averaged by a boxcar system (a PAR Model 162 boxcar averager and a PAR Model 155 gated integrator). The aperture duration τ_g, aperture delay τ_d,, and time constant τ_c used for the boxcar averager will be described in the table and figure legends. The overall rise time was about 2 μs. The signal picked up by a photon drag detector was used as the trigger for the boxcar averager. The flow rate of a reactant gas in the cell was set between 1 and 10 Torr ml min^{-1} according to the pressure used. Pressures were measured with a capacitance-type manometer (MKS Baratron Model 220 BH).

Fluoroethane was synthesized through reaction of potassium fluoride with ethyl tosylate and purified by low temperature distillation.[11] Its purity was found to be higher

than 99% in an infrared absorption measurement. Argon purchased from Takachiho Kagaku Kogyo Co. (research grade) was used without further purification.

Results

The laser irradiation of 9.0 Torr C_2H_5F at a fluence of 40 J cm^{-2} yielded infrared fluorescence in a wide wavelength region of 2.2—3.8 μm. The spectrum of Fig. 1 (a) in the region of 2.2—3.2 μm (solid curve) is attributed to vibrationally excited HF*. The observed spectrum was simulated according to the method reported by Quick and Wittig.[8] The rotation-vibration terms of HF* were calculated by using the equation[12]

$$F_{vJ} = \sum_{lm} Y_{lm}(v+1/2)^l[J(J+1)]^m, \quad (1)$$

where Y_{lm} is a constant related to the molecular constants of HF; J and v are a rotational quantum number and a vibrational quantum number, respectively. On the other hand, the emission intensity of the v', $J'\rightarrow v''$, J'' transition I_{em} was calcualted by using the equation

$$I_{em} \propto \frac{C_{em}\,\nu^4\,F\,S_{J'}}{Q_r}\exp\left[-(F_{v'J'} - F_{v'0})(hc)/(kT)\right], \quad (2)$$

where $S_{J'}$ is $J'+1$ for P branch, *i.e.* $\Delta J=J'-J''=-1(J'=0, 1, 2, \cdots)$ and J' for R branch, *i.e.*, $\Delta J=+1$ ($J'=1, 2, 3, \cdots$); C_{em} is a constant proportional to the square of a transition dipole moment, values for various vibrational transitions being given in the paper by Herblin and Emanuel;[13] the symbol ν is a transition frequency; Q_r is the rotational partition function defined by a certain rotational temperature T; the Boltzmann distribution being assumed for the rotational level populations; F is a relative vibrationa level population, which may be regarded as a fitting parameter in this simulation; the symbols h and k are the Planck and Boltzmann constants, respectivery; and c is the light speed. Finally, each profile of emission line was determined from the slit function and the simulation spectrum was constructed by superposing the emission lines. The

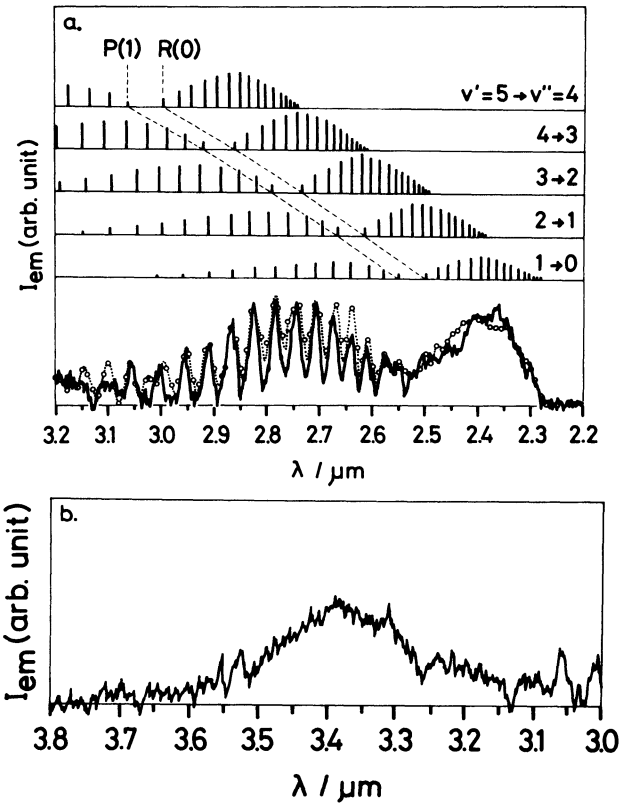

Fig. 1. Infrared fluorescence spectra obtained with CO_2 TEA laser irradiation of 9.0-Torr C_2H_5F in the wavelength regions of 2.2—3.2 (a) and 3.0—3.8 μm (b). Irradiation wavenumber, 1046.85 cm^{-1}; laser fluence, 40 J cm^{-2}; wavelength resolution, 0.016 μm fwhm; τ_d, 1 μs; τ_g, 10 μs (see Experimental). Relative emission intensities of rotation-vibration transitions ($\Delta v=1$ and $v'\leqq 5$) are shown in the upper part, where T_{rot} is assumed to be 1800 K. O, calculated point (see text).

Table 1. Pressure effects on rotational temperatures and vibrational level populations of HF* produced in IRMPD of C_2H_5F[a]

C_2H_5F	Ar	T_{rot}	N_{vib}				
Torr	Torr	K	$v'=1$	2	3	4	5
0.025	1.5	300	1	0.50	0.40	0.10	0
0.05	3.0	300	1	0.50	0.40	0.10	0.10
0.10	5.9	300	1	0.60	0.40	0.10	0.10
0.17	9.8	300	1	0.50	0.30	0.10	0
0.28		800	1	0.60	0.40	0.20	0
0.40		800	1	0.60	0.40	0.10	0
0.50		900	1	0.50	0.30	0.10	0
1.0		900	1	0.40	0.15	0.30	0.05
2.0		1000	1	0.30	0.05	0.30	0
5.0		1500	1	0.33	0.13	0.25	0.19
		(±300)		(±0.08)	(±0.08)	(±0.11)	(±0.11)
6.0		1800	1	0.35	0.05	0.30	0
9.0		1800	1	0.25	0.05	0.35	0.25
0.20[b]	12(He)	450	1	0.60	0.25	0.10	0
				(±0.1)	(±0.05)		
0.20[b]		800	1	0.55	0.2	0.1	0

a) Laser line, 9.6 μm P(20) at 1046.85 cm^{-1}; laser fluence, approximately 40 J cm^{-2} (E_{in}=0.23 J pulse^{-1} and focal length=20 cm); τ_d=1 μs; τ_g=10 μs. b) Ref. 8.

calculated intensity distributions of the rotational lines due to the rotation-vibration transitions ($\Delta v=1$ and $v' \leqq 5$) with a common rotational temperature of 1800 K are illustrated in the upper part of Fig. 1(a), where each vibrational level has the same total population. Then, the fluorescence intensities through the actual slit function, which had a triangular shape with 0.016 μm fwhm, were calculated at wavelength intervals of 0.01 μm, as shown by the open circles in Fig. 1(a). The vibrational level populations were selected so that the simulated spectrum gave the best fit. The dotted curve represents a smooth connection of the calculated points. Figure 1(b) is the fluorescence spectrum in the region of 3.0—3.8 μm, which may originate from vibrationally excited parent molecules $C_2H_5F^*$ because the emission center at about 3.4 μm coincides in wavelength with the $v'=1 \leftarrow v''=0$ transition in the C-H stretching mode of C_2H_5F. The ratio of the emission peak intensity of HF* (at 2.35 μm) to that of $C_2H_5F^*$ (at 3.4 μm) is about 1.3.

The variation in pressure influences the rotational temperature T_{rot} and vibrational level populations N_{vib} of HF*; the pressure effects on T_{rot} and N_{vib} are summarized in Table 1. These data were obtained from the spectral simulation where N_{vib} ($v'=1$) was always normalized to unity in each case. Both T_{rot} and N_{vib} are fitting parameters in the present treatment. T_{rot} can be estimated directly from the spectral shape in the wavelength region below 2.36 μm since the rotational lines of the $v'=1 \rightarrow v''=0$ transition are isolated from those of the other transitions. For 5.0-Torr C_2H_5F the simulation was performed for four spectra observed independently under the same experimental conditions. The error limit in Table 1 shows the range of the scatter of T_{rot} or N_{vib} in the simulation. In practice, we could not satisfactorily reproduce the spectrum obtained with 5.0-Torr C_2H_5F by using the values out of the error limits. Quick and Wittig[8] gave error limits, which are included in Table 1 for the vibrational level populations calculated in a similar manner. The rotational temperature increases with an increase in C_2H_5F pressure. When the partial pressure of C_2H_5F was lower than 0.17 Torr, argon approximately 60 times was added to the system. The addition of argon to a reaction mixture lowers T_{rot} to room temperature and enhances the signal intensity, *i.e.*, the dissociation probability, while N_{vib} at each vibrational level is scarcely affected by the addition of argon. The effect of argon is also shown in Table 1, where N_{vib} at each vibrational level has similar values for C_2H_5F at 0.025—0.50 Torr with and without argon, although T_{rot} changes between 300 and 900 K. For comparison, the populations reported by Quick and Wittig[8] are included in the same table; their result is consistent with ours.

Figure 2 presents four typical HF* fluorescence spectra obtained at different pressures, where open circles are calculated in the above-mentioned method. The wavelength resolution was sacrificed for the measurements at low pressures because the emission intensity decreased with decreasing pressure. The spectrum apparently becomes broader with increasing pressure above 0.5 Torr. The relative fluorescence intensities due to HF* at $v'=2$ and 3 decrease with increasing pressure, while those due to $v'=4$ and 5 increase. T_{rot} also increases with pressure. It is worth noting that the absolute fluorescence intensities due to HF* and $C_2H_5F^*$ increase markedly with an increase in C_2H_5F pressure. However, the intensity due to $C_2H_5F^*$ grows more rapidly as compared with that due to HF*.

The infrared fluorescence spectra determined at 3, 10, 20, 30, and 50 μs after the laser pulse are shown in

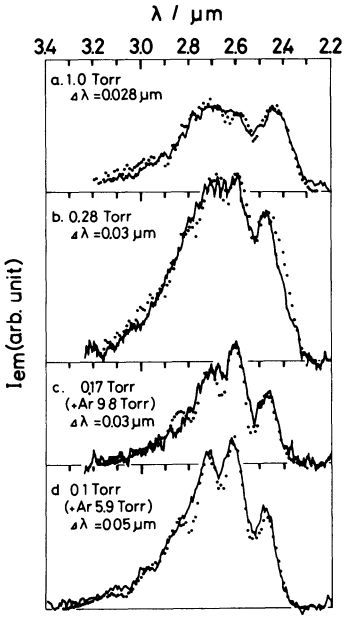

Fig. 2. Infrared fluorescence spectra obtained with 1.0-Torr (a), 0.28-Torr (b), 0.17-Torr (c), and 0.1-Torr (d) C_2H_5F. Argon was added in (c) and (d). Laser fluence, 40 J cm^{-2}; τ_d, 1 μs; τ_g, 10 μs; O, calculated point. Wavelength resolution Δλ is shown in the figure.

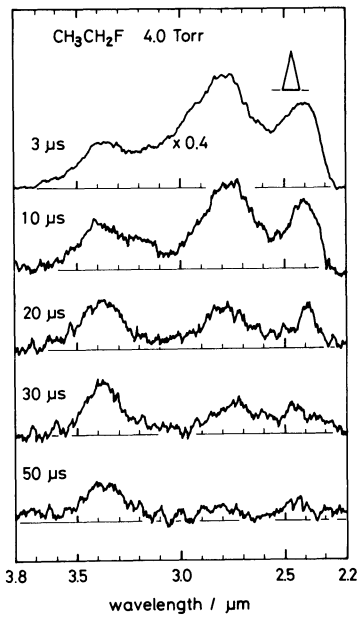

Fig. 3. Infrared fluorescence spectra obtained with 4.0-Torr C_2H_5F. The spectra were determined at 3, 10, 20, 30, and 50 μs after the laser pulse. Wavelength resolution is shown in the figure. Laser fluence, 40 J cm^{-2}; τ_d, 1 μs; τ_g, 10 μs.

Table 2. Transient vibrational populations of HF* produced in IRMPD of C_2H_5F[a)]

τ_d	T_{rot}	N_{vib}				
μs	K	$v'=1$	2	3	4	5
2	1800	1	0.4	0.2	0.2	0.3
3	1800	1	0.4	0.2	0.1	0.3
6	1200	1	0.3	0.05	0.4	0.1
10	1200	1	0.2	0.05	0.3	0.05
15	1200	1	0.2	0.05	0.15	0.05
20	1200	1	0.2	0.05	0.15	0.05

a) Laser line, 9.6 μm P(20) (1046.85 cm^{-1}); laser fluence, about 40 J cm^{-2}; τ_g=1 μs; C_2H_5F pressure, 5.0±0.1 Torr.

Fig. 3. The pressure of C_2H_5F is 4.0 Torr. The time dependences of the vibrational level populations obtained with 5.0-Torr C_2H_5F are summarized in Table 2. The vibrational level populations at v'=2, 3, and 5 decrease with a lapse of time; the higher the level is, the larger is the decrease. The population at v'=4 reaches a maximum at 6 μs and then decreases.

Table 3 presents the fluence effect on the fluorescence. The production of HF* at high vibrational levels tends to increase with increasing fluence. This tendency can be seen with 5-Torr C_2H_5F alone and with the mixture of 0.17-Torr C_2H_5F and 9.83-Torr Ar. However, the change in vibrational level population is not evident in the present study because a possible fluence variation is restricted within a narrow range.

Figure 4 shows the fluorescence intensity *vs.* time curve observed at 2.4, 2.8, and 3.4 μm for 4-Torr C_2H_5F. The fluorescence monitored at 2.4 μm corresponds mainly to the R branch of the HF* (v'=1)→HF(v''=0) transition, while that at 2.8 μm includes several transitions of Δv=1 from various vibrational levels. Parent molecules fluoresce at the vicinity of 3.4 μm. The fluoresce due to HF* grows almost completely within the response time of the detection system, *i.e.*, 3 μs. The following decay consists of the rapid component with a lifetime of 10 μs and the slow component lasting for 30—40 μs. The whole temporal behavior is invariant against C_2H_5F pressure if it is higher than 0.5 Torr. In contrast, only the slow component is observed for the decay curve if the pressure is lower than 0.2 Torr. Moreover, the decay rate tends to decrease with decreasing pressure in the low pressure region.

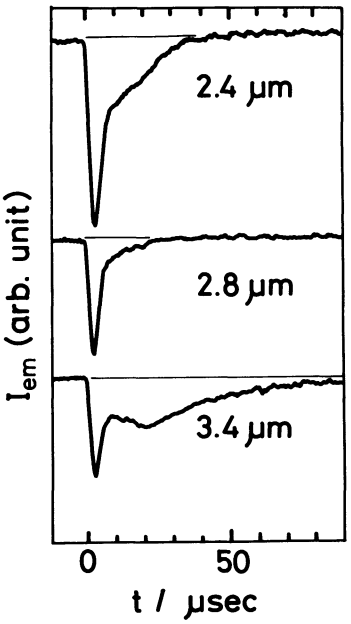

Fig. 4. Fluorescence intensity *vs.* time curves obtained with 4.0-Torr C_2H_5F. Laser fluence, 40 J cm^{-2}.

Discussion

Setser and coworkers[14)] and Quick and Wittig[8)] have reported that the molecular elimination of HF occurs in IRMPD of C_2H_5F:

$$C_2H_5F + nh\nu \longrightarrow C_2H_4 + HF$$
$$\Delta H = 10 \text{ kcal mol}^{-1}. \quad (4)$$

The activation energy of this reaction has been found to be approximately 57 kcal mol^{-1}. The dissociation energies of bonds C–C, C–H, and C–F in ethane-type molecules are estimated to be 85, 100, and 100 kcal mol, respectively. Therefore, the molecular elimination of HF should be the most favorable reaction channel in IRMPD of C_2H_5F. When 4.0 Torr C_2H_5F was irradiated with a CO_2 TEA laser (1000 pulses), three new bands attributable to products appeared near 1030, 950, and 730 cm^{-1} in the infrared absorption spectrum. The first band corresponds to the ν_3 mode (SiF deg. stretch) of SiF_4,[15)] the second to the ν_7 mode (CH_2 wag) of C_2H_4,[16)] and the third to the ν_5 mode (CH bend) of C_2H_2.[16)] Acetylene may be formed secondarily by the

Table 3. Laser fluence effect on the vibrational populations of HF* in IRMPD of C_2H_5F[a)]

Laser fluence	T_{rot}	N_{vib}					
J cm^{-2}	K	v'=1	2	3	4	5	6
[C_2H_5F]=5.0±0.1 Torr[b)]							
20	1800	1	0.7	0.1	0.4	0	0
23	2000	1	0.7	0.1	0.2	0.2	0
24	2000	1	0.8	0.2	0.3	0.3	0
29	2000	1	0.4	0.05	0.2	0.4	0
40	2000	1	0.4	0.05	0.1	0.5	0.2
[C_2H_5F]=0.17 Torr and [Ar]=9.8 Torr[c)]							
30	300	1	0.2	0.4	0.2	0	
36	300	1	0.8	0.6	0.1	0	
41	300	1	0.8	0.6	0.1	0.1	
46	300	1	0.8	0.6	0.3	0.2	

a) Laser line, 9.6 μm P(20) (1046.85 cm^{-1}). b) τ_d=3 μs and τ_g=1 μs. c) τ_d=1 μs and τ_g=5 μs.

decomposition of ethylene.[17] The production of SiF_4 implies that hydrogen fluoride reacts with the glass wall. These results support the previous conclusion that Reaction (4) proceeds most efficiently in IRMPD of C_2H_5F. We could not find the infrared emission due to vibrationally excited DF* in IRMPD of a mixture of 1-Torr C_2H_5F and 2-Torr D_2. This fact suggests that no fluorine atom is produced in the primary process of IRMPD of C_2H_5F.

Vibrational level populations have been estimated for hydrogen halides produced from halogenated hydrocarbons activated in various processes. Steady-state infrared fluorescences of hydrogen halides were measured in chemical activation[18] and mercury sensitized photolysis.[19] Transient fluorescences were measured in UV laser photolysis.[20] Throughout these measurements, N_v was always larger than N_{v+1}. In the present study, however, we found the extraordinary population distribution of HF* at C_2H_5F pressures higher than 1.0-Torr. The extraordinary population distribution might be explained in the following ways: (a) some vibrational levels of HF* are overpopulated in the so-called Treanor distribution *via* collisional V-V ladder climbing;[21] (b) the energy transfer from highly vibrationally excited C_2H_5F* yields preferentially HF* at some particular vibrational levels. Fürsich and Kompa[22] could not observe any inverted vibrational population when hydrogen fluoride at 30—60 Torr was directly excited with pulses from a high power HF laser. This result denies item (a) above as a reasonable cause for the extraordinary population distribution. In our experiment, pressures of C_2H_5F are lower than 10 Torr. Since HF is produced from excited C_2H_5F*, the partial pressure of vibrationally excited hydrogen fluoride HF* should be much lower than 10 Torr. It is highly improbable that the Treanor distribution of HF* is accomplished at low partial pressures of HF. Vibrationally excited C_2H_5F* was found to fluoresce in the wavelength region of 3.1—3.6 μm. As shown in Figs. 3 and 4, the fluorescence was observed over 100 μs after the pulse, although the fluorescence due to HF* terminated within 40 μs. The clear difference between the transient behavior of C_2H_5F* and HF* seems to rule out item (b) above for the production of HF*.

The fluorescence intensity *vs.* time curve observed at 2.4 μm for 0.17-Torr of C_2H_5F exhibits only one decay component, which fits a first-order kinetic low. The origin of HF* at such a low pressure may be the laser-induced multiple-photon decomposition of C_2H_5F. The collision-induced process can be ignored for the production of HF*. Assuming that HF* is fully produced within the pulse duration, one can estimate the rate constant for the collisional deactivation of HF* to be $3\times10^5\,s^{-1}\,Torr^{-1}$. The fluorescence monitored at 2.4 μm is due to HF* in a vibrational state of $v'=1$. Hancock and Green[23] have measured rate constants of deactivation of HF* ($v'=1$) by several hydrocarbons by use of the laser-induced vibrational fluorescence technique. Of the rate constants, cyclopropane has the same value as C_2H_5F.

The HF* fluorescence intensity *vs.* time curves obtained with C_2H_5F at pressures higher than 0.5 Torr show a fast rise followed by fast and slow decays. The qeunching lifetime of HF* is expected to be shorter than 1 μs if the pressure of C_2H_5F is higher than 3 Torr. The initial fluorescence spike is mainly due to the HF* molecules produced in IRMPD of C_2H_5F. The fast rise is limited by the response time of the detection system since the production of HF* in IRMPD terminates at the end of pulse. The fast decay is caused by the collisional deactivation of the fraction of HF* produced in IRMPD. The slow decay suggests that HF* is also produced in a slow process after the termination of pulse. One possible mechanism for the slow formation of HF* is the decomposition of excited C_2H_5F molecules produced in the collision induced process. The direct IRMPE of C_2H_5F results in the distribution of excited molecules over a wide range of internal energy. Those C_2H_5F molecules which have energies much higher than the threshold energy undergo immediate decomposition. On the other hand, those molecules which have energies almost euqal to or a little higher than the threshold energy persist for a long time after the laser pulse irradiation. It should be noted that the reaction zone in IRMPD is limited to a small volume around a focal point and that most molecules in the reaction zone are in highly vibrationally excited states. Collisions among vibrationally excited molecules with long lifetimes may produce excited molecules above the dissociation threshold. The excited HF* molecules formed in the subsequent decomposition may show the inverted vibrational level populations. The energy distribution of excited C_2H_5F molecules approaches the Boltzmann distribution defined by temperature with a lapse of time. However, the fraction of excited molecules produced above the threshold during the relaxation process undergoes the decomposition leading to the formation of HF*. The temperature inside a reaction zone is usually high enough to induce thermal decomposition in IRMPD at high fluences or high pressures. However, the temperature gradually decreases as excited molecules diffuse from the reaction zone or cold molecules diffuse into the reaction zone.

A pressure is expected to affect IRMPD through hole filling and energy transfer. These phenomena couple together to influence the absorption and decomposition processes. Richardson and Setser[14] have studied IRMPD of binary mixtures, where one component does not absorb the laser energy but does possess the decomposition channel with the threshold energy comparable to that of the other component. The decomposition yields of both components were measured as a function of total pressure. They found that for pressures $\geq$1 Torr the intermolecular energy transfer is sufficiently rapid that the collision-induced decomposition of the non-absorbing molecule is prominent. In our experiment, the collision-induced decomposition seems to become important for pressures $\geq$1 Torr.

The response time and sensitivity of the present detection system are not satisfactory for transient infrared fluorescence observation. Therefore, it is exceedingly difficult to separate out the effects of the collision-induced process on the observed vibrational level populations from those arising from the laser-induced multiple-photon excitation process itself. However, we observed the distribution of HF* with $N_v/N_{v+1}\geq1$ at low pres-

sures of C_2H_5F where IRMPD occurs mainly. The extraordinary distribution becomes more prominent with increasing pressure or a lapse of time. These facts are consistent with the above-mentioned mechanism.

References

1) R. V. Ambartzumian, N. V. Chekalin, V. S. Dolzhikov, V. S. Letokhov, and E. A. Ryabov, *Chem. Phys. Lett.*, **25**, 515 (1974); R. V. Ambartzumian, V. S. Dolzhikov, V. S. Letokhov, E. A. Ryabov, and N. V. Chekalin, *Sov. Phys.-JETP*, **42**, 36 (1976).

2) R. Corkum, C. Willis, and R. A. Back, *Chem. Phys.*, **24**, 13 (1977).

3) Y. Haas and G. Yahav, *Chem. Phys. Lett.*, **48**, 63 (1977); G. Yahav and Y. Haas, *Chem. Phys.*, **35**, 41 (1978).

4) C. R.Quick, Jr., J. J. Tiee, T. A. Fischer, and C. Wittig, *Chem. Phys. Lett.*, **62**, 435 (1979).

5) W. C. Danen and J. C. Jang, "Multiphoton Infrared Excitation and Reaction of Organic Compounds," in "Laser-Induced Chemical Processes," ed by J. L. Steinfeld, Plenum Press, New York (1981), p. 117.

6) S. L. Baughcum and S. R. Leone, *J. Chem. Phys.*, **72**, 6531 (1980); M. G. Moss, M. D. Ensminger, and J. D. McDonald, *J. Chem. Phys.*, **74**, 6631 (1981).

7) G. A. West, R. E. Weston, Jr., and G..W. Flynn, *Chem. Phys.*, **35**, 275 (1978); C. R. Quick, Jr. and C. Wittig, *ibid.*, **32**, 75 (1978); C. R. Quick, Jr. and C. Wittig, *J. Chem. Phys.*, **69**, 4201 (1978).

8) C. R. Quick, Jr. and C. Wittig, *J. Chem. Phys.*, **72**, 1694 (1980).

9) Y. Ishikawa, H. Yamazaki, Y. Hama, and S. Arai, *Appl. Phys.*, **B32**, 85 (1983).

10) C. M. Miller and R. N. Zare, *Chem. Phys. Lett.*, **71**, 376 (1980).

11) W. F. Edgell and L. Parbs, *J. Am. Chem. Soc.*, **77**, 4899 (1955).

12) D. U. Webb and K. N. Rao, *J. Mol. Spectrosc.*, **28**, 121 (1968).

13) J. M. Herbelin and G. Emanuel, *J. Chem. Phys.*, **60**, 687 (1974).

14) T. H. Richardson and D. W. Setser, *J. Phys. Chem.*, **81**, 2301 (1977); J. C. Jang and D. W. Setser, *J. Phys. Chem.*, **83**, 2809 (1979).

15) E. A. Jones, J. S. Kirby-Smith, P. J. H. Woltz, and A. M. Nielsen, *J. Chem. Phys.*, **19**, 242 (1951).

16) T. Shimanouchi, "Tables of Molecular Vibrational Frequencies Consolidated Volume I," NSRDS-NBS 39, (1972).

17) N. C. Peterson, R. G. Manning, and W. Braun, *J. Res. NBS*, **83**, 117 (1977).

18) M. J. Berry and G. C. Pimentel, *J. Chem. Phys.*, **49**, 5190 (1968); M. J. Berry and G. C. Pimentel, *IEEE J. Quantum Electron.*, **QE-6**, 176 (1970); P. N. Clough, J. C. Polanyi, and R. T. Taguchi, *Can. J. Chem.*, **48**, 2919 (1970).

19) H. Watanabe, H. Horiguchi, and S. Tsuchiya, *Bull. Chem. Soc. Jpn.*, **53**, 1530 (1980).

20) M. J. Berry, *J. Chem. Phys.*, **61**, 3114 (1974).

21) C. E. Treanor, J. W. Rich, and R. G. Rehm, *J. Chem. Phys.*, **48**, 1798 (1968).

22) M. Fürsich and K. L. Kompa, *J. Chem. Phys.*, **75**, 763 (1981).

23) J. K. Hancock and W. H. Green, *J. Chem. Phys.*, **59**, 6350 (1973).